

3

4 **Roles of the cumulus-oocyte transzonal network and the Fragile X protein family**
5 **in oocyte competence**

6

7 Elolo Karen Nenonene^{1,2,3}, Mallorie Trottier-Lavoie^{1,2,3}, Mathilde Marchais^{1,2,3},
8 Alexandre, Bastien^{1,2,3}, Isabelle Gilbert^{1,2,3}, Angus D Macaulay^{1,2}, Edouard W
9 Khandjian⁴, Alberto Maria, Luciano⁵, Valentina Lodde⁵, Robert Viger^{6,2,3}, Claude
10 Robert^{1,2,3*}

11 **Affiliations**

12 ¹ Département des sciences animales, Faculté des sciences de l'agriculture et de
13 l'alimentation;

14 ² Centre de Recherche en Reproduction, Développement et Santé Intergénérationnelle
15 (CRDSI);

16 ³ Réseau Québécois en Reproduction (RQR), Université Laval, Québec, Québec,
17 Canada ⁴ Centre de recherche CERVO, Département de psychiatrie et de
18 neurosciences, Faculté de médecine, Université Laval, Québec, Québec, Canada

19 ⁵ Reproductive and Developmental Biology Laboratory, Department of Veterinary
20 Medicine and Animal Science, University of Milan, Milan, Italy

21 ⁶ Département d'obstétrique, gynécologie et reproduction, Faculté de médecine,
22 Université Laval, Québec, Québec Canada

23 ***Correspondence** : Faculté des sciences de l'agriculture et de l'alimentation,
24 Département des sciences animales, Pavillon Paul Comtois, 2425, Rue de

25 l'Agriculture, Québec, Canada, G1V 0A6, Tel: 418-656-2131, Email :
26 claire.robert@fsaa.ulaval.ca

27 **Short title:** Transzonal projections and FXRPs in oocytes

28 **Keywords:** Transzonal projection, RNA-binding protein, Fragile X-Related Proteins,
29 Ribonucleoprotein, Oocyte competence

30
31 **In brief:** RNA granules travel through the cumulus cell network of transzonal
32 projections which is associated with oocyte developmental competence and RNA
33 packaging involves RNA binding proteins of the Fragile X protein family.

34

35 **Abstract**

36 The determinants of oocyte developmental competence have puzzled scientists
37 for decades. It is known that follicular conditions can nurture the production of a high-
38 quality oocyte, but the underlying mechanisms remain unknown. Somatic cumulus
39 cells most proximal to the oocyte are known to have cellular extensions that reach
40 across the zona pellucida and contact with the oocyte plasma membrane. Herein, it
41 was found that transzonal projections (TZPs) network quality is associated with
42 developmental competence. Knowing that ribonucleo-particles are abundant within
43 TZPs, the distribution of RNA binding proteins were studied. The Fragile X-Related
44 Proteins (FMRP, FXR1P, and FXR2P) and two partnering protein families, namely
45 cytoplasmic FMRP interacting protein (CYFIP) and nuclear FMRP interacting protein
46 (NUFIP), exhibited distinctive patterns consistent with roles in regulating mRNA
47 packaging, transport and translation. Expression of GFP-FMRP fusion protein in
48 cumulus cells showed active granule formation and their transport and transfer through
49 filipodia connecting with neighboring cells. Near the projections' ends was found the
50 cytoskeletal anchoring protein Filamin A and active protein synthesis sites. This study

51 highlights key proteins involved in delivering mRNA to the oocyte. Thus, cumulus
52 cells appear to indeed support the development of high-quality oocytes via the
53 transzonal network.

54

55 **Introduction**

56 Oocyte quality can be defined simply as the competency to resume meiosis, be
57 fertilized, and undergo development to a stage beyond the activation of the embryonic
58 genome, at which point the blastomeres acquire some ability to adjust independently
59 to the surrounding environment. This definition focuses on the time interval spanning
60 the embryonic program, which begins with gamete preparation during oogenesis,
61 concurrent with folliculogenesis. Bovine oocytes acquire the potential to resume
62 meiosis when they reach full size in antral follicles at about 3 mm in diameter (Fair *et al.*,
63 1995). *In vitro* culture has shown clearly that most embryo lethality occurs before
64 embryonic genome activation (Plourde *et al.*, 2012; Dieci *et al.*, 2016) and that
65 developmental competence is affected by conditions experienced by the oocyte during
66 the later stages of folliculogenesis (Nivet *et al.*, 2012).

67 Folliculogenesis is a highly regulated process in which the different cell types
68 comprising the ovarian follicle are interdependent and work as a syncytium. Our main
69 interest is in the close relationship between the gamete and its surrounding somatic
70 cells, maintained throughout folliculogenesis even after the glycoprotein shell or zona
71 pellucida is secreted (Anderson and Albertini, 1976; Gilula *et al.*, 1978). Cumulus cells
72 maintain physical contact with the oocyte by extending cellular processes through this
73 shell. We have shown that ribonucleoprotein complexes of considerable size transit
74 through these transzonal channels (Macaulay *et al.*, 2014; Macaulay *et al.*, 2016).
75 However, the mechanisms that control mRNA transit remain unknown. Using a
76 pulldown assay for *de novo* synthesized transcripts found inside the channels, several

77 genes potentially associated with mRNA shuttling were identified at the top of this list
78 and Fragile X-Related Proteins (FXRPs) were found (Macaulay *et al.*, 2014). This
79 group of proteins is composed of Fragile X Multi-Role Protein (also known as Fragile
80 X Mental Retardation Protein) (FMRP), Fragile X Related Protein 1 (FXR1P) and
81 Fragile X Related Protein 2 (FXR2P). Therefore, we hypothesize that an extensive
82 network of transzonal channels is a hallmark of a competent oocyte and that the
83 proteins involved in carrying mRNA include FXRPs.

84 The role of FXRPs in the ovary has not been fully explored, even though the
85 correlation with female reproductive lifespan was shown long ago (Schwartz *et al.*,
86 1994; Vianna-Morgante *et al.*, 1996; Murray *et al.*, 1998; Sullivan *et al.*, 2005). In
87 human, *FMR1* (coding for FMRP) acquired a destabilizing sequence in the form of
88 repeating CGG trinucleotides inserted within the location corresponding to the 5' UTR
89 of the mRNA. This sequence is subject to expansion during DNA replication.

90 Perturbations in *FMR1* leading to lower FMRP expression is associated with a
91 decrease in female reproductive lifespan, causing about 20% of women to develop
92 Fragile X-Associated Primary Ovarian Insufficiency (FXPOI) (Murray *et al.*, 1998;
93 Sherman, 2000; Wheeler *et al.*, 2014). The most important symptom of the FXPOI
94 syndrome is reaching menopause before the age of 40 due to early depletion of oocyte
95 stocks (De Caro *et al.*, 2008; Gleicher *et al.*, 2014; Jiao *et al.*, 2018). The premutation
96 is known to result in lower levels of FMRP that impacts oocyte competence through a
97 yet unknown mechanism.

98 FMRP is known to interact *in vitro* with other members of the FXRPs family,
99 which include the FXR1 and FXR2 proteins (FXR1P and FXR2P) (Zhang *et al.*, 1995).
100 In neurons, these proteins form complexes that can bind mRNA to form granules,

101 which are involved in mRNA transport and the control of translation (Davidovic *et*
102 *al.*, 2007; Graber *et al.*, 2013; El Fatimy *et al.*, 2016). FMRP also interacts with the
103 cytoplasmic FMR1-interacting protein (CYFIP) and the nuclear FMRP interacting
104 protein (NUFIP) families (Bardoni *et al.*, 1999; Schenck *et al.*, 2001). Proteins of the
105 CYFIP family are responsible for cytoskeleton remodeling and are involved with
106 FMRP in the extension of actin-based cytoplasmic projections such as dendrites (De
107 Rubeis *et al.*, 2013; Pathania *et al.*, 2014; Hsiao *et al.*, 2016). By contrast, those of the
108 NUFIP family are either nuclear and bind only to the specific nuclear FMRP isoform
109 12 or cytoplasmic RNA-binding proteins that localize with ribosomes and FMRP
110 (Bardoni *et al.*, 1999; Bardoni *et al.*, 2003).

111 This study aimed to assess whether an association exists between the transzonal
112 network, members of the FXRPs family and its interacting partners, and oocyte
113 developmental competence. Therefore, localization of FMRP, FXR1P, FXR2P,
114 CYFIP1, CYFIP2 and NUFIP1 within the transzonal projections (TZPs) was
115 performed to observe their possible involvement in mRNA transport from cumulus
116 cells to the oocyte. We found that the target proteins were abundant within TZPs under
117 the form of granules consistent with mRNA packaging, transport, and translation.
118 Also, active protein synthesis sites were found at the edge of the oocyte plasma
119 membrane near and overlapping the tips of TZPs.

120

121 **Material and Methods**

122 *Ethics statement*

123 This project was evaluated and approved by the Animal Care Council of Laval
124 University. The research project does not involve the use of animals dedicated for the
125 purposes of this project. Cattle and pig ovaries were collected at different
126 slaughterhouses during their normal operation. For Figure 1, ovaries from Holstein

127 dairy cows were recovered at the abattoir INALCA S.p.A., Ospedaletto Lodigiano,
128 LO, IT 2270M CE, Italy. For other figures, cow ovaries were collected at Abattoir
129 Bolduc, Buckland, QC, Canada. Pig ovaries were collected at the Olymel SEC
130 slaughterhouse, Vallée-Jonction, QC, Canada. All animals and slaughterhouses
131 facilities are subjected to routine veterinary inspection and operate in accordance with
132 the specific health requirements stated in Council Directive 89/556/ECC and
133 subsequent modifications (Italy) and under the legislation and supervision of the
134 Canadian Food Inspection Agency (Canada). Tissue collection did not alter the normal
135 flow of events at the slaughterhouses including animal demise and post-mortem
136 processing. This study did not require handling animals on university premises.

137

138 *Ovary collection*

139 Ovaries from dairy cows aged four to eight years and from prepubertal gilts were
140 collected in local slaughterhouses. Ovaries were placed immediately in a warm saline
141 solution (0.9% NaCl) containing of an antimycotic antibiotic (Sigma-Aldrich,
142 Oakville, ON, Canada) and were maintained at 37°C (bovine) or 34°C (porcine) during
143 transport.

144 *Oocyte collection*

145 Ovaries were rinsed twice in the saline solution. Cumulus-oocyte complexes (COC)
146 were collected by aspirating visible follicles between 3 and 6 mm in diameter and were
147 placed in a 50 ml Falcon flask. COC selection based on morphology was carried out
148 in phosphate-buffered saline solution with polyvinyl alcohol (PBS-PVA). Only
149 oocytes with three or more compact layers of cumulus cells and homogeneous
150 cytoplasm were included in the study (n = 20 oocytes per group). Bovine oocytes from
151 high-efficiency or low-efficiency ovaries were categorized based on the number of
152 antral follicles in the 3–6 mm size range visible in the ovarian cortex, as described

153 previously (Modina *et al.*, 2007; Modina *et al.*, 2014). This categorization was used as
154 a proxy variable for bovine oocyte developmental competence.

155 *Immunofluorescence*

156 Complete description of the antibodies used in this study can be found in Supplemental
157 Table S1. Immunolocalization was performed as described previously (Macaulay *et*
158 *al.*, 2014; Macaulay *et al.*, 2016). Selected COCs were denuded partially by repeatedly
159 drawing them into a pipette. The resulting oocytes were fixed for 10 min in 4%
160 paraformaldehyde in PBS-PVA and permeabilized for 20 min in 1% Triton X-100.
161 Non-specific sites were blocked using 5% bovine serum albumin for 1 h. Incubation
162 with primary antibody was for at least 16 h at 4°C. Oocytes were then washed 3 times
163 for 5 min each at room temperature and incubated for 1 h with a 1:1000 dilution of
164 secondary antibody: Alexa-Fluor 488 goat anti-rabbit, Alexa-Fluor 555 goat anti-
165 rabbit (ThermoFisher Scientific, Waltham, MA, USA) or Alexa-Fluor 488 goat anti-
166 chicken (Biotium, San Francisco, CA, USA). After three washings for 5 min each, the
167 oocytes were incubated with 1.5% actin stain 670 Phalloidin (Cytoskeleton, Denver)
168 for actin filament detection and Hoechst dye 33342 (Invitrogen, product no. H21492)
169 diluted 1:1000 for DNA staining. Controls with nonimmune primary antibody and
170 secondary antibody were run in parallel.

171 172 *TZP network quality assessment*

173 Using the actin staining, TZPs are highlighted and imaged. Ten images spaced 1 μm
174 apart at the equator of the oocyte are taken to make a maximum intensity projection
175 (MIP). TZPs are handdrawn, and the intensity values are the average of the value of
176 the pixels that has been identified (drawn) as part of a TZP. We use a 16-bit detector
177 and measurements can take a value between 0 and 65,535. An in-house developed

178 script is used to output an intensity value, a length and a straightness value for
179 each TZP. The script is available here:

180 [https://github.com/alexandrebastien/ImageJ-Script-](https://github.com/alexandrebastien/ImageJ-Script-Collection/blob/master/ULaval_Misc1.0.0/scripts/Plugins/ULaval/TZPs_Analyzer.ijm)
181 [Collection/blob/master/ULaval_Misc1.0.0/scripts/Plugins/ULaval/TZPs_Analyzer.ij](https://github.com/alexandrebastien/ImageJ-Script-Collection/blob/master/ULaval_Misc1.0.0/scripts/Plugins/ULaval/TZPs_Analyzer.ijm)
182 [m](https://github.com/alexandrebastien/ImageJ-Script-Collection/blob/master/ULaval_Misc1.0.0/scripts/Plugins/ULaval/TZPs_Analyzer.ijm)

183 *Candidate protein detection*

184 Primary antibodies against FMRP and FXR1 have been described previously (Mazroui
185 *et al.*, 2002; El Fatimy *et al.*, 2012). Anti-FXR2 (Atlas antibodies, Stockholm,
186 Sweden), anti-CYFIP1 (Thermo-Fisher Scientific) anti-NUFIP1 (Thermo-Fisher
187 Scientific) were used at 1 µg/ml, antiCYFIP2 (Thermo-Fisher Scientific) at 2 µg/ml,
188 and anti-Filamin A (Sigma-Aldrich) at 1% (vol.).

189 Cell transfection

190 Intact COCs were matured *in vitro* for 22 h using standard maturation medium as
191 previously described (Plourde *et al.*, 2012). Cumulus cells were stripped from matured
192 COCs by gently pipetting and plated in six-well plates at a concentration of 1.5-2
193 million cells per mL in DMEM (Life Technologies, Burlington, ON, Canada)
194 supplemented with sodium bicarbonate (MP Biomedial, Santa Anna, CA, USA),
195 bovine albumin (Sigma), Fugizone (Life Technologies). Cells were left in culture for
196 3-5 days prior to two transfections one day apart. Plasmid delivery was carried out
197 with the TransIT X2 system from Mirus (Madison, WI, USA). The construct was done
198 in the pcDNA 3.1 (+) plasmid (Life Technologies) containing eGFP and human *FMRI*
199 cDNA producing a functional fusion protein (Davidovic *et al.*, 2007). Time-lapse
200 microscopy was conducted 12 h post-transfection.

201

202 *Live-cell and time-lapse imaging*

203 RNA granules were tracked *in vivo* using Syto RNASelect green-fluorescent cell stain
204 solution (Thermo-Fisher Scientific) prewarmed to 37°C. Selected COCs and partially

205 denuded oocytes were incubated for 30 min in 5 μ M of Syto RNASelect green-
206 fluorescent cell stain solution (Thermo-Fisher Scientific). They were then rinsed twice
207 for 5 min in culture medium, placed immediately in maturation medium in 280 μ m
208 diameter wells in a custom-made dish. Video recording was done using a Zeiss Live-
209 Cell LSM700 confocal microscope in a humidified atmosphere at 37°C with 5% CO₂.
210 Images of transzonal projections were taken at 40X while images of transfected
211 cumulus cell culture were taken at 10X and 20X. All images were captured using ZEN
212 software at several intervals ranging from 1.5 to 50 seconds.

213 *Active translation*

214 Active translation was detected using a commercial kit (Click-iT Plus OPP Alexa Fluor
215 488 Protein Synthesis Assay Kit, Thermo-Fisher Scientific). Selected COCs were
216 labeled by incubation with 100 μ l of Click-iT OPP reagent at 20 mM for 30 min at
217 37°C. Complexes were then washed once in PBS and fixed with 4% paraformaldehyde
218 for 15 min. Fixed COCs were permeabilized for 15 min in 0.5% Triton X-100 at room
219 temperature, washed twice in 100 μ l of PBS and mixed with 100 μ l of Click-iT Plus
220 OPP reaction cocktail (prepared according to the manufacturer's protocol with 1X
221 Click-iT reaction buffer in deionized water and 1X Click-iT reaction buffer additive)
222 for 30 min at 37°C away from light. COCs were then removed from the reaction
223 mixture and washed once in 100 μ l of Click-iT reaction rinse buffer.

224 *Data analysis*

225 Immunofluorescence images were analyzed using ImageJ software to determine
226 oocyte fluorescence intensity and corresponding TZPs total length and to localize foci
227 of the protein of interest. Transzonal characteristic means were compared using
228 Student's t-test while protein foci means were compared using one-way ANOVA with

229 the Tukey post hoc test for Fragile X-Related Proteins family or Student's t-test for
230 CYFIP family members. Statistical significance was set at $p < 0.05$. JASP software
231 was used for statistical analysis. Each group contained $n = 15$ oocytes.

232

233 **Results**

234 Using visual follicle count, oocytes were collected from High quality ovaries
235 (more than 10 follicles of 2 to 5 mm in diameter) and Low-quality ovaries (less than
236 10 follicles) as published previously (Modina *et al.*, 2007; Tessaro *et al.*, 2011; Modina
237 *et al.*, 2014). This allowed for the production of two groups of oocytes with contrasting
238 developmental potentials. It has been shown that high-quality oocytes, as defined in
239 these studies, reach the blastocyst stage *in vitro* $32.2 \pm 1.9\%$ of the time versus $8.2 \pm$
240 1.2% of the time for the corresponding low-quality oocytes (Modina *et al.*, 2007).
241 Based on fluorescent intensity, oocytes recovered from high-efficiency ovaries had a
242 significantly better developed transzonal network ($p < 0.001$) than those from low-
243 efficiency ovaries (Figure 1A). The TZPs tended to be longer overall ($p = 0.087$) in
244 oocytes recovered from high-efficiency ovaries (Figure 1B).

245 Our interest being in the transport of mRNA cargos within TZPs, labeling of total
246 RNA combined with live-cell time-lapse image tracking showed the presence of
247 granules sent from the cumulus cell body into the TZPs (Figure 2). Granular movement
248 appeared to be mostly towards the oocyte with little reflux. We also noted that the
249 granules appeared to be larger as they approached the entrance to the zona pellucida
250 (Figure 2). In the zona pellucida, Fragile X-Related Proteins family only showed minor
251 differences in distribution (Figures 3). In oocytes, FMRP, FXR1P and FXR2P
252 overlapped with the TZP actin cytoskeleton (Figure 3). However, the general
253 distribution patterns of the FXRPs differed (Figure 3). FMRP foci were found in
254 majority in the first half of the zona pellucida closer to the cumulus cells (Figure 3).

255 The majority of FXR2P foci were also found in the first half of the zona but more on
256 the outskirts which coincides with the beginning of the TZPs (Figure 3), while FXR1P
257 foci were found throughout the zona pellucida and along the entire length of the
258 projections (Figure 3). This suggests distinctive roles for the FXRPs in RNA
259 packaging, transport and control. FXRPs and partner proteins abundance and
260 distribution within cumulus-oocyte complexes might be a conserved trait in view of
261 the similar results obtained for porcine FMRP (Supplemental Figure 1) and FXR2P
262 (Supplemental Figure 1). A few foci were detectable throughout the projections with
263 FXR1P again being uniformly distributed (Supplemental Figure 1).

264 The cytoplasmic FMRP interacting proteins CYFIP1 and CYFIP2 have a very
265 different distribution in bovine oocytes even though both occur in granular form in the
266 cytoplasm and in the surrounding cumulus cells (Figure 4). Both are known to interact
267 with FXRPs. CYFIP1 foci spanned the entire TZP length like strings of pearls and
268 produced larger foci in the first half of the zona (Figure 4). CYFIP2 foci were present
269 in the cytoplasm of cumulus cells but in a distinctly granular form inside projections
270 (Figure 4). They were partial to the outer half of the zona pellucida much like FMRP
271 and FXR2P.

272 The distributions of porcine CYFIP1 and CYFIP2 foci were also similar to the
273 bovine case. CYFIP1 (Supplemental Figure 2) had the same string-of-pearls-like
274 arrangement and appeared more abundant than CYFIP2, with foci close to the
275 oolemma.

276 The nuclear-interacting FMR proteins, NUFIP1 and NUFIP2, were also
277 associated with newly synthesized mRNA transcripts in cumulus cells and found
278 previously in TZPs (Macaulay *et al.*, 2014). This was not expected since these partner
279 proteins are better known for their localization in the nuclear compartment. As

280 anticipated, NUFIP1 was very abundant in all bovine cumulus cell nuclei but
281 surprisingly, extra-nuclear foci were found throughout TZPs including in the bulging
282 ends (Figure 5). The NUFIP1 signal was more diffuse in the oocyte cytoplasm. In
283 porcine, the distribution of NUFIP1 was also very similar to that in bovine COCs with
284 foci abundant throughout the projections and in the end bulb (Supplemental Figure 3).

285 To show that FMRP can actively generate granules that can be carried through
286 cellular extensions, cumulus cells were cultured and transfected with a plasmid
287 containing a GFP-FMRP sequence generating a functional fusion protein (Davidovic
288 *et al.*, 2007). Transfection efficiency was about 25%. Typically, cumulus cells extend
289 filipodia to neighboring cells connecting each other. Cells expressing the construct
290 contained abundant GFP-FMRP granules that moved along the cellular extensions
291 similarly to the RNA granules detected in transzonal projections. Transfer of GFP-
292 FMRP granules was observed where delivery was done from a transfected cell to
293 another that was not expressing the construct (Figure 6). The figure shows a large
294 fluorescent granule disappearing within the cell's cytoplasm and two additional
295 granules that were tracked to move toward and to be delivered to the receiving cell
296 (Figure 6 side panels).

297 Since FXRPs and their interacting proteins are known to be involved in binding,
298 packaging, transporting and controlling the translation of mRNA in neurons
299 (Khandjian *et al.*, 2004; Stefani *et al.*, 2004; Darnell *et al.*, 2011; El Fatimy *et al.*,
300 2016), they are also known as being involved in the development of the neuronal
301 network. In the present study, we localized Filamin A (FLNA), a candidate protein
302 found in neurons and proven to interact with FMRP (Bolduc *et al.*, 2010). FLNA is a
303 known anchoring molecule that interacts with the actin filament and cell surface
304 membrane glycoproteins such as integrins (Li *et al.*, 1999). Consistent with its known

305 roles, FLNA was detected mainly at the base of TZPs where the cumulus cell and
306 oocyte membranes are juxtaposed (Figure 7).

307 Cumulus cell mRNA sent through the transzonal network in complexes with
308 RNA-binding FXRPs and related partners must be released and translated locally for
309 projection development and maintenance purposes or transferred to the oocyte via
310 synapse-like vesicular secretion as shown previously (Macaulay *et al.*, 2014; Macaulay
311 *et al.*, 2016). Using a fluorescent amino acid analog, no active translation was detected
312 along the projection length, confirming the repressed state of the mRNA during
313 transport. However, numerous hubs of active translation were found near and
314 overlapping the projection end bud (Figure 8). Results in this study as whole shed light
315 on, at least, part of the mechanism by which cumulus cell mRNA is packed then
316 transported through TZPs to where they are released for translation.

317 **Discussion**

318 The factors that control oocyte quality are multifactorial and complex. In this
319 study, we sought to better understand the role of transzonal network quality. We also
320 show an mRNA transport system in which the FXRPs and partners participate. In the
321 first perspective, we hypothesized that a poorly developed transzonal network could
322 have a negative impact on oocyte quality. We tested this hypothesis using a model of
323 developmental competence where ovaries with signs of reduced antral follicle count
324 produce low developmental competence oocytes (Modina *et al.*, 2007; Tessaro *et al.*,
325 2011). The present results indicate that these low-quality oocytes harbor an
326 underdeveloped transzonal network. This agrees with other reports using different
327 models of oocyte developmental competence where lower number of TZPs are found
328 in COCs from smaller size follicles in mouse (El-Hayek and Clarke, 2015) and COCs
329 of gilts under heat stress harbor less TZPs (Yin *et al.*, 2020). This suggests that
330 conditions during folliculogenesis can modulate the quality of the transzonal network,

331 which in turn could reduce the overall support from cumulus cells essential for the
332 acquisition of developmental competence.

333 Cumulus cells are known to nurture the oocyte through the network of TZPs by
334 providing cyclic nucleotides which control meiotic resumption (Gilchrist *et al.*, 2016)
335 as well as energetic substrates which palliate to an inefficient glycolytic pathway in
336 the oocyte (Sutton-McDowall *et al.*, 2010; Richani *et al.*, 2021). Recently, we have
337 demonstrated that the projections also actively deliver mRNA to the oocyte (Macaulay
338 *et al.*, 2014; Macaulay *et al.*, 2016). This mRNA transfer appears to be important for
339 developmental competence. Indeed, in bovine COCs, TZPs are not constantly loaded
340 with RNA. The timeframe of RNA accumulation in these channels, while the COCs
341 are still enclosed in follicles, coincides with acquisition of developmental competence.
342 In the case of COCs recovered from slaughterhouse ovaries, the timing of aspiration
343 post mortem was found to be a determinant of developmental competence: waiting for
344 4 hours before COCs collection increases blastocyst formation to $30.5 \pm 1.9\%$ versus
345 $14.7 \pm 0.5\%$ after 2 hours (Blondin *et al.*, 1997). Under these conditions, RNA
346 accumulation in transzonal projections was also found to peak at 4 hours before COCs
347 retrieval (Macaulay *et al.*, 2016). In this model of developmental competence, the
348 quality of the TZP network cannot be a factor since neither oocyte morphology nor the
349 number of TZPs differs. Taken together, this supports the notion that a low-quality
350 network and reduced network activity can both negatively impact oocyte
351 developmental competence.

352 Based on this evidence suggesting that oocyte competence requires delivery of
353 mRNA from cumulus cells, we next sought to investigate how this transfer occurs. As
354 we previously reported (Macaulay *et al.*, 2014; Macaulay *et al.*, 2016), and again
355 shown here, mRNAs are shuttled in granules across TZPs. FXRPs were selected as

356 candidates from an initial survey of newly synthesized transcripts found in bovine
357 cumulus cells and TZPs (Macaulay *et al.*, 2014; Macaulay *et al.*, 2016).

358 Also, the involvement of one member of the FXRPs, namely FMRP, has been
359 demonstrated in women fertility where a reduced expression significantly increases
360 the risk of experiencing menopause before the age of 40 (Schwartz *et al.*, 1994;
361 Vianna-Morgante *et al.*, 1996; Murray *et al.*, 1998; Sullivan *et al.*, 2005). This
362 phenotype has been described as a normal pool of primordial follicles followed by
363 growth-impaired follicles and, finally, an extensive presence of atretic follicles
364 (Hoffman *et al.*, 2012; Lu *et al.*, 2012). The molecular mechanism through which the
365 RNA binding protein impacts oogenesis and follicular demise has not yet been
366 described. However, knock-out mouse models with *Fmr1* or *Fxr2* inactivated
367 individually have not been associated with specific reproductive phenotypes (The
368 Dutch-Belgian Fragile X Consortium, 1994; Bontekoe *et al.*, 2002) while *Fxr1-KO* is
369 non-viable (Mientjes *et al.*, 2004).

370 Our results indicate that all three FXRPs are present in TZPs in an evolutionary
371 conserved manner. Moreover, the *in vitro* transfection assay reported here confirms
372 FMRP can form granules that can be carried and transferred to neighboring cumulus
373 cells. In both bovine and porcine COCs, there is a great presence of FXR1P granules
374 along the TZPs while FMRP was mostly found on the outskirts of the zona with fewer
375 granules along the TZPs. FXR2P was mostly restricted to the outskirts of the zona
376 corresponding to the origin of the projections. Since all three FXR proteins contribute
377 to the formation of messenger ribonucleoprotein complexes for silencing and transport
378 of mRNA (Graber *et al.*, 2013; El Fatimy *et al.*, 2016), FMRP and FXR2P are likely

379 involved in silencing of mRNA as it enters the projections whereas FXR1P is more
380 involved in the active shuttling.

381 We also detected CYFIP1 and CYFIP2, which are not mRNA-binding but
382 rather actinremodeling proteins able to interact with FMRP (Schenck *et al.*, 2001;
383 Pathania *et al.*, 2014). CYFIP1-containing granules appeared to be abundant
384 throughout the transzonal network whereas CYFIP2 occurred mostly in the outer two
385 thirds of the zona. Previous studies have shown that the absence of CYFIP1 in the
386 brain is associated with decreased actin-based cytoplasmic protrusions and increased
387 translation of certain other proteins (Napoli *et al.*, 2008; Bozdagi *et al.*, 2012;
388 Abekhoukh *et al.*, 2017). These protein partnerships seem necessary for the
389 structuration of the cytoskeleton involved in cellular extensions.

390 Also found with FXRPs is NUFIP1, an mRNA-binding protein that associates
391 with FMRP (Bardoni *et al.*, 2003). NUFIP1 is a nucleocytoplasmic mRNA-shuttling
392 protein from the nucleus where it is found adjacent to active transcription sites and in
393 the cytoplasm in association with ribosomes (Bardoni *et al.*, 2003). In most cell types,
394 NUFIP1 is mainly nuclear (Bardoni *et al.*, 2003; Nabart *et al.*, 2004). In the present
395 study, while NUFIP1 was not found in oocytes, it was found unexpectedly abundant
396 in TZPs, suggesting the presence of ribosomes and mRNP complexes supporting its
397 role in mRNA transport from cumulus cells to the oocyte.

398 The roles of FXRPs and partner proteins in packaging and transporting mRNA
399 and regulating translation imply remote protein synthesis, which could be necessary to
400 establish and maintain the transzonal network and transfer mRNA and/or proteins to

401 the oocyte. One candidate for the network building and maintenance function is a
402 protein that we had previously noted, namely filamin A (FLNA), a cross-linking
403 protein known to anchor actin filaments to membrane glycoproteins (Li *et al.*, 1999).
404 Interaction between FLNA and FMRP has been reported in *Drosophila*. In FMR1-
405 knock-out animals, FLNA is downregulated, which may cause the characteristic thin
406 and elongated appearance of dendritic spines (Bolduc *et al.*, 2010). Since FLNA is a
407 major constituent of intercellular connectivity, its inactivation has major life-impairing
408 consequences, including decreased female fertility (Li *et al.*, 1999; Feng *et al.*, 2006).
409 Murine studies have shown FLNA enrichment of the cortex from the germinal vesicle
410 to the MII stages and that knockdown decreases cytoplasmic actin mesh and cortical
411 actin content (Wang *et al.*, 2017). In the present study, FLNA was predominantly
412 found around the tip of TZPs, suggesting that it plays a role in maintaining contact
413 between cumulus cells and the oocyte. In addition, detection of active translation sites
414 has confirmed the presence of distal protein synthesis localized in the same area near
415 the ends of TZPs. Standard fluorescent confocal microscopy does not have sufficient
416 resolution to precisely position the signal to determine if it is exclusively within the
417 tip of TZPs or adjacent to it in the oocyte cortex. Both are not mutually exclusive.
418 Nonetheless, our data clearly show active translation sites closely localized to the
419 projections' end supporting the translation of transported mRNAs.

420 In conclusion, we propose that the development and functionality of the
421 transzonal network is an essential determinant of oocyte competence. Our observations
422 constitute evidence that in addition to small molecules, mRNA is transported from
423 cumulus cells to the oocyte through the network and that FXRPs and NUFIP1 are
424 likely involved. The abundance and distribution of these proteins individually support
425 distinctive roles in mRNA packaging and transport. Translation sites were detected at
426 the distal end of TZPs. Although the results do not confirm that amongst the mRNAs

427 being translated are some originating from the cumulus cells, we speculate that
428 cumulus cells provide proteins to the oocyte in a controlled manner. The proposed
429 transport mechanism appears to operate in porcine as well as bovine cumulus-oocyte
430 complexes. Conditions that decrease FMRP expression would result in decreased
431 CYFIP1 activity and decreased FLNA expression, which would lead to less
432 connectivity between cumulus cells and the oocyte and hence an overall reduction of
433 physiological support for the oocyte.

434 **Declaration of interest**

435 The authors have no conflict of interest to disclose.

436 **Funding**

437 Natural Sciences and Engineering Research Council of Canada (Grant RGPIN-2017-
438 04775) and Fonds Québécois de la Recherche sur la Nature et les Technologies (Grant
439 182922).

440 **Author contribution statement**

441 E.K.N., M.T.L., M.M., A.B. performed the experiments. E.K.N. and IG drafted the
442 manuscript. E.W.K. provided the custom antibodies and GFP-FMRP expression
443 vectors, A.M.L. and V.L. provided the high and low quality ovaries. ADM generated
444 the time-lapse data of Fig 6. C.R. designed and supervised the study. E.W.K., A.M.L,
445 V.L., R.V. and C.R. performed critical revision of the manuscript. All authors have
446 given approval for publication of the present version of this manuscript.

447 **Acknowledgements**

448 The authors want to thank Isabelle Laflamme and Karine Dubuc for their technical
449 expertise and support. We also thank Dr Shlomit Kenigsberg from the Juno Fertility

450 Clinic, Toronto, Canada for her valuable input regarding Filamin A and Dr Laetitia
451 Davidovic from the CNRS - Institute of Molecular and Cellular Pharmacology, Nice,
452 France and Dr Michael Tranfaglia from the FRAXA Research Foundation, USA for
453 discussing the new nomenclature of FMRP.

454

References

- 457 Abekhoukh S, Sahin HB, Grossi M, Zongaro S, Maurin T, Madrigal I, Kazue-Sugioka D,
458 RaasRothschild A, Doulazmi M, Carrera P *et al.* (2017) New insights into the
459 regulatory function of CYFIP1 in the context of WAVE- and FMRP-containing
460 complexes. *Disease Models & Mechanisms* 10 463–474.
- 461 Anderson E and Albertini DF (1976) Gap junctions between the oocyte and companion follicle
462 cells in the mammalian ovary. *The Journal of Cell Biology* 71 680–686.
- 463 Bardoni B, Schenck A and Louis Mandel J (1999) A Novel RNA-binding Nuclear Protein
464 That Interacts With the Fragile X Mental Retardation (FMR1) Protein. *Human*
465 *Molecular Genetics* 8 2557–2566.
- 466 Bardoni B, Willemsen R, Weiler IJ, Schenck A, Severijnen L-A, Hindelang C, Lalli E and
467 Mandel J-L (2003) NUFIP1 (nuclear FMRP interacting protein 1) is a
468 nucleocytoplasmic shuttling protein associated with active synaptoneurosome.
469 *Experimental Cell Research* 289 95–107.
- 470 Blondin P, Coenen K, Guilbault LA and Sirard MA (1997) In vitro production of bovine
471 embryos: developmental competence is acquired before maturation. *Theriogenology*
472 47 1061–1075.
- 473 Bolduc FV, Bell K, Rosenfelt C, Cox H and Tully T (2010) Fragile x mental retardation 1
474 and filamin a interact genetically in Drosophila long-term memory. *Frontiers in*
475 *Neural Circuits* 3 22.
- 476 Bontekoe CJM, McIlwain KL, Nieuwenhuizen IM, Yuva-Paylor LA, Nellis A, Willemsen
477 R, Fang Z, Kirkpatrick L, Bakker CE, McAninch R *et al.* (2002) Knockout mouse
478 model for Fxr2: a model for mental retardation. *Human Molecular Genetics* 11 487–
479 498.
- 480 Bozdagi O, Sakurai T, Dorr N, Pilorge M, Takahashi N and Buxbaum JD (2012)
481 Haploinsufficiency of Cyfip1 Produces Fragile X-Like Phenotypes in Mice. *PLoS*
482 *ONE* 7.
- 483 ▀abart P, Chew HK and Murphy S (2004) BRCA1 cooperates with NUFIP and P-TEFb to
484 activate transcription by RNA polymerase II. *Oncogene* 23 5316–5329.
- 485 Darnell JC, Van Driesche SJ, Zhang C, Hung KY, Mele A, Fraser CE, Stone EF, Chen C,
486 Fak JJ, Chi SW *et al.* (2011) FMRP stalls ribosomal translocation on mRNAs linked
487 to synaptic function and autism. *Cell* 146 247–261.
- 488 Davidovic L, Jaglin XH, Lepagnol-Bestel A-M, Tremblay S, Simonneau M, Bardoni B and
489 Khandjian EW (2007) The fragile X mental retardation protein is a molecular
490 adaptor between the neurospecific KIF3C kinesin and dendritic RNA granules.
491 *Human Molecular Genetics* 16 3047–3058.
- 492 De Caro JJ, Dominguez C and Sherman SL (2008) Reproductive health of adolescent girls
493 who carry the FMR1 premutation: expected phenotype based on current knowledge

- 494 of fragile x-associated primary ovarian insufficiency. *Annals of the New York*
495 *Academy of Sciences* 1135 99–111.
- 496 De Rubeis S, Pasciuto E, Li KW, Fernández E, Di Marino D, Buzzi A, Ostroff LE, Klann E,
497 Zwartkruis FJT, Komiyama NH *et al.* (2013) CYFIP1 Coordinates mRNA
498 Translation and Cytoskeleton Remodeling to Ensure Proper Dendritic Spine
499 Formation. *Neuron* 79 1169–1182.
- 500 Dieci C, Lodde V, Labreque R, Dufort I, Tessaro I, Sirard M-A and Luciano AM (2016)
501 Differences in cumulus cell gene expression indicate the benefit of a pre-maturation
502 step to improve in-vitro bovine embryo production. *Molecular Human Reproduction*
503 22 882– 897.
- 504 El Fatimy R, Tremblay S, Dury AY, Solomon S, De Koninck P, Schrader JW and Khandjian
505 EW (2012) Fragile mental retardation protein interacts with the RNA-binding protein
506 Caprin1 in neuronal RiboNucleoProtein complexes. *PloS One* 7 e39338.
- 507 El Fatimy R, Davidovic L, Tremblay S, Jaglin X, Dury A, Robert C, De Koninck P
508 and
509 Khandjian EW (2016) Tracking the Fragile X Mental Retardation Protein in a Highly
510 Ordered Neuronal RiboNucleoParticles Population: A Link between Stalled
511 Polyribosomes and RNA Granules. *PLoS Genetics* 12 e1006192.
- 512 El-Hayek S and Clarke HJ (2015) Follicle-Stimulating Hormone Increases Gap Junctional
513 Communication Between Somatic and Germ-Line Follicular Compartments During
514 Murine Oogenesis. *Biology of Reproduction* 93 47.
- 515 Fair T, Hyttel P and Greve T (1995) Bovine oocyte diameter in relation to maturational
516 competence and transcriptional activity. *Molecular Reproduction and Development*
517 42 437–442.
- 518 Feng Y, Chen MH, Moskowitz IP, Mendonza AM, Vidali L, Nakamura F, Kwiatkowski DJ
519 and Walsh CA (2006) Filamin A (FLNA) is required for cell-cell contact in vascular
520 development and cardiac morphogenesis. *Proceedings of the National Academy of*
521 *Sciences of the United States of America* 103 19836–19841.
- 522 Gilchrist RB, Luciano AM, Richani D, Zeng HT, Wang X, Vos MD, Sugimura S, Smitz J,
523 Richard FJ and Thompson JG (2016) Oocyte maturation and quality: role of cyclic
524 nucleotides. *Reproduction (Cambridge, England)* 152 R143-157.
- 525 Gilula NB, Epstein ML and Beers WH (1978) Cell-to-cell communication and ovulation. A
526 study of the cumulus-oocyte complex. *Journal of Cell Biology* 78 58–75.
- 527 Gleicher N, Kushnir VA, Weghofer A and Barad DH (2014) How the FMR1 gene became
528 relevant to female fertility and reproductive medicine. *Front Genet* 5.
- 529 Graber TE, Hébert-Seropian S, Khoutorsky A, David A, Yewdell JW, Lacaille J-C and
530 Sossin WS (2013) Reactivation of stalled polyribosomes in synaptic plasticity. *PNAS*
531 110 16205–16210.
- 532 Hoffman GE, Le WW, Entezam A, Otsuka N, Tong Z-B, Nelson L, Flaws JA, McDonald JH,

- 533 Jafar S and Usdin K (2012) Ovarian Abnormalities in a Mouse Model of Fragile X
534 Primary Ovarian Insufficiency. *Journal of Histochemistry & Cytochemistry* 60 439–
535 456.
- 536 Hsiao K, Harony-Nicolas H, Buxbaum JD, Bozdagi-Gunal O and Benson DL (2016) Cyfip1
537 Regulates Presynaptic Activity during Development. *The Journal of Neuroscience* 36
538 1564–1576.
- 539 Jiao X, Ke H, Qin Y and Chen Z-J (2018) Molecular Genetics of Premature Ovarian
540 Insufficiency. *Trends in Endocrinology & Metabolism* 29 795–807.
- 541 Khandjian EW, Huot M-E, Tremblay S, Davidovic L, Mazroui R and Bardoni B (2004)
542 Biochemical evidence for the association of fragile X mental retardation protein with
543 brain polyribosomal ribonucleoparticles. *Proceedings of the National Academy of
544 Sciences* 101 13357–13362.
- 545 Li M, Serr M, Edwards K, Ludmann S, Yamamoto D, Tilney LG, Field CM and Hays TS
546 (1999) Filamin Is Required for Ring Canal Assembly and Actin Organization during
547 *Drosophila* Oogenesis. *Journal of Cell Biology* 146 1061–1074.
- 548 Lu C, Lin L, Tan H, Wu H, Sherman SL, Gao F, Jin P and Chen D (2012) Fragile X
549 premutation RNA is sufficient to cause primary ovarian insufficiency in mice.
550 *Human Molecular Genetics* 21 5039–5047.
- 551 Macaulay AD, Gilbert I, Caballero J, Barreto R, Fournier E, Tossou P, Sirard M-A, Clarke
552 HJ, Khandjian EW, Richard FJ *et al.* (2014) The Gametic Synapse: RNA Transfer to
553 the Bovine Oocyte1. *Biology of Reproduction* 91.
- 554 Macaulay AD, Gilbert I, Scantland S, Fournier E, Ashkar F, Bastien A, Saadi HAS, Gagné
555 D, Sirard M-A, Khandjian EW *et al.* (2016) Cumulus Cell Transcripts Transit to the
556 Bovine Oocyte in Preparation for Maturation. *Biology of Reproduction* 94.
- 557 Mazroui R, Huot M-E, Tremblay S, Filion C, Labelle Y and Khandjian EW (2002) Trapping
558 of messenger RNA by Fragile X Mental Retardation protein into cytoplasmic
559 granules induces translation repression. *Human Molecular Genetics* 11 3007–3017.
- 560 Mientjes EJ, Willemsen R, Kirkpatrick LL, Nieuwenhuizen IM, Hoogeveen-Westerveld M,
561 Verweij M, Reis S, Bardoni B, Hoogeveen AT, Oostra BA *et al.* (2004) Fxr1
562 knockout mice show a striated muscle phenotype: implications for Fxr1p function in
563 vivo. *Human Molecular Genetics* 13 1291–1302.
- 564 Modina S, Borromeo V, Luciano AM, Lodde V, Franciosi F and Secchi C (2007)
565 Relationship between growth hormone concentrations in bovine oocytes and
566 follicular fluid and oocyte developmental competence. *European Journal of
567 Histochemistry: EJH* 51 173–180.
- 568 Modina SC, Tessaro I, Lodde V, Franciosi F, Corbani D and Luciano AM (2014) Reductions
569 in the number of mid-sized antral follicles are associated with markers of premature
570 ovarian senescence in dairy cows. *Reproduction, Fertility and Development* 26 235.
- 571 Murray A, Webb J, Grimley S, Conway G and Jacobs P (1998) Studies of FRAXA and
572 FRAXE in women with premature ovarian failure. *Journal of Medical Genetics* 35
573 637–640.

- 574 Napoli I, Mercaldo V, Boyl PP, Eleuteri B, Zalfa F, De Rubeis S, Di Marino D, Mohr E,
575 Massimi M, Falconi M *et al.* (2008) The Fragile X Syndrome Protein Represses
576 ActivityDependent Translation through CYFIP1, a New 4E-BP. *Cell* 134 1042–
577 1054.
- 578 Nivet A-L, Bunel A, Labrecque R, Belanger J, Vigneault C, Blondin P and Sirard M-A
579 (2012) FSH withdrawal improves developmental competence of oocytes in the
580 bovine model. *Reproduction (Cambridge, England)* 143 165–171.
- 581 Pathania M, Davenport EC, Muir J, Sheehan DF, López-Doménech G and Kittler JT (2014)
582 The autism and schizophrenia associated gene CYFIP1 is critical for the maintenance
583 of dendritic complexity and the stabilization of mature spines. *Translational*
584 *Psychiatry* 4 e374–e374.
- 585 Plourde D, Vigneault C, Laflamme I, Blondin P and Robert C (2012) Cellular and molecular
586 characterization of the impact of laboratory setup on bovine in vitro embryo
587 production. *Theriogenology* 77 1767-1778.e1.
- 588 Richani D, Dunning KR, Thompson JG and Gilchrist RB (2021) Metabolic co-dependence
589 of the oocyte and cumulus cells: essential role in determining oocyte developmental
590 competence. *Human Reproduction Update* 27 27–47.
- 591 Schenck A, Bardoni B, Moro A, Bagni C and Mandel J-L (2001) A highly conserved protein
592 family interacting with the fragile X mental retardation protein (FMRP) and
593 displaying selective interactions with FMRP-related proteins FXR1P and FXR2P.
594 *Proceedings of the National Academy of Sciences of the United States of America* 98
595 8844–8849.
- 596 Schwartz CE, Dean J, Howard-Peebles PN, Bugge M, Mikkelsen M, Tommerup N, Hull C,
597 Hagerman R, Holden JJA and Stevenson RE (1994) Obstetrical and gynecological
598 complications in fragile X carriers: A multicenter study. *American Journal of*
599 *Medical Genetics* 51 400–402.
- 600 Sherman SL (2000) Premature ovarian failure in the fragile X syndrome. *Am J Med Genet* 97
601 189–194.
- 602 Stefani G, Fraser CE, Darnell JC and Darnell RB (2004) Fragile X mental retardation protein
603 is associated with translating polyribosomes in neuronal cells. *The Journal of*
604 *Neuroscience* 24 7272–7276.
- 605 Sullivan AK, Marcus M, Epstein MP, Allen EG, Anido AE, Paquin JJ, Yadav-Shah M and
606 Sherman SL (2005) Association of FMR1 repeat size with ovarian dysfunction.
607 *Human Reproduction* 20 402–412.
- 608 Sutton-McDowall ML, Gilchrist RB and Thompson JG (2010) The pivotal role of glucose
609 metabolism in determining oocyte developmental competence. *Reproduction*
610 *(Cambridge, England)* 139 685–695.
- 611 Tessaro I, Luciano AM, Franciosi F, Lodde V, Corbani D and Modena SC (2011) The
612 endothelial nitric oxide synthase/nitric oxide system is involved in the defective
613 quality of bovine oocytes from low mid-antral follicle count ovaries. *Journal of*
614 *Animal Science* 89 2389–2396.

- 615 The Dutch-Belgian Fragile X Consortium (1994) Fmr1 knockout mice: a model to study
616 fragile X mental retardation. The Dutch-Belgian Fragile X Consortium. *Cell* 78 23–
617 33.
- 618 Vianna-Morgante AM, Costa SS, Pares AS and Verreschi ITN (1996) FRAXA premutation
619 associated with premature ovarian failure. *American Journal of Medical Genetics* 64
620 373–375.
- 621 Wang H, Guo J, Lin Z, Namgoong S, Oh JS and Kim N (2017) Filamin A is required for
622 spindle migration and asymmetric division in mouse oocytes. *The FASEB Journal* 31
623 3677–3688.
- 624 Wheeler AC, Bailey DB, Berry-Kravis E, Greenberg J, Losh M, Mailick M, Milà M,
625 Olichney JM, Rodriguez-Reventa L, Sherman S *et al.* (2014) Associated features in
626 females with an FMR1 premutation. *J Neurodev Disord* 6.
- 627 Yin C, Liu J, Chang Z, He B, Yang Y and Zhao R (2020) Heat exposure impairs porcine
628 oocyte quality with suppressed actin expression in cumulus cells and disrupted F-
629 actin formation in transzonal projections. *Journal of Animal Science and*
630 *Biotechnology* 11 71.
- 631 Zhang Y, O'Connor JP, Siomi MC, Srinivasan S, Dutra A, Nussbaum RL and Dreyfuss G
632 (1995) The fragile X mental retardation syndrome protein interacts with novel
633 homologs FXR1 and FXR2. *The EMBO Journal* 14 5358–5366.
- 634

636 **Figure legends**

637 **Figure 1. Correlation between transzonal network development and oocyte**
638 **quality.** Bovine ovaries were classified as high-efficiency or low-efficiency based on
639 ovarian morphology (Modina *et al.*, 2007). (A) Ovaries with a morphology associated
640 with COCs leading to better embryonic rates exhibit a greater brightness in their TZPs
641 (AU, Arbitrary Unit ($p < 0.001$)). (B) TZPs tended to be longer overall in oocytes from
642 high efficiency ovaries ($p = 0.087$).

643 **Figure 2. Progress of an RNA granule through the zona pellucida (ZP) from a**
644 **bovine cumulus cell towards the oocyte.** Live-cell imaging shows the movement of
645 an RNA granule (purple arrow) for an average 12 sec period for each picture. Total
646 RNA was stained with Syto RNASelect and is represented by the cyan blue color, Oo,
647 oocyte; ZP, zona pellucida, CC, cumulus cells. Scale bar = 20 μm .

648 **Figure 3. Different localization of the Fragile X-Related Proteins in transzonal**
649 **projections (TZPs) of bovine cumulus oocyte-complexes (COCs).**
650 Immunofluorescence confocal microscopy images showing the actin filament of the
651 TZP (red) and the presence of A) FMRP, B) FXR1P and C) FXR2P within TZPs
652 (green). Actin filaments of TZPs were stained with Acti-stain 670 phalloidin (red);
653 primary antibodies against FMRP, FXR1P and FXR2P were subsequently incubated
654 with secondary antibodies conjugated with Alexa Fluor 488 (green). Scale bars = 20
655 μm .

656 **Figure 4. Distribution of the cytoplasmic interacting family of FMR proteins 1**
657 **and 2 (CYFIP1 and CYFIP2) in bovine cumulus-oocyte complexes (COCs).**
658 Immunofluorescence confocal microscopy images showing the actin filament of the
659 TZP (red) and the localization of A) CYFIP1 and B) CYFIP2 in TZPs (green). TZPs
660 were stained with Acti-stain 670 phalloidin (red). Primary antibodies against CYFIP1,
661 and CYFIP2 were subsequently incubated with secondary antibodies conjugated with
662 Alexa Fluor 488 (green). Scale bars = 20 μ m.

663

664 **Figure 5. Distribution of nuclear interacting FMR protein 1 (NUFIP1) in bovine**
665 **cumulusoocyte complexes (COCs).** Immunofluorescence confocal microscopy
666 images showing the actin filament of the TZP (red) and the localization of NUFIP1
667 (green) within the TZPs in bovine COCs.
668 TZPs were stained with acti-stain 670 phalloidin (red). DNA was stained with Hoechst
669 33432 dye (blue). Scale bars = 20 μ m.

670 **Figure 6. GFP-FMRP expression in bovine cumulus cells.** Cultured cumulus cells
671 were transfected with a construct generating a GFP-FMRP fusion protein. Mobile
672 green fluorescent granules were detected in the cells' filipodia. Side panels represent
673 a time-lapse sequence in seconds showing the transfer of a large granule to the
674 cytoplasm of the neighboring non-transfected cell (white arrow head) as well as the
675 tracking of two other granules. In the yellow rings, coalescing of GFP-puncta into a
676 larger granule is observed. The same phenomenon is observed in the red rings, and the
677 fused puncta migrates to the neighbor cell situated in the top of the images. Scale bar=
678 20 μ m.

679 **Figure 7. Detection of filamin A (FLNA) at the junction of oocyte membrane and**
680 **cumulus cells in a bovine oocyte.** Immunofluorescence confocal microscopy showing
681 localization of
682 FLNA in transzonal projection (TZP) actin. TZPs were visualized using Acti-stain 670
683 Phalloidin (red); Primary antibodies against FLNA were subsequently incubated with
684 secondary antibodies conjugated with Alexa Fluor 488 (blue). Scale bar = 20 μm .

685 **Figure 8. *De novo* translation of mRNA in a bovine oocyte.** FXR1P (green) was
686 stained with Alexa Fluor 555; *de novo* translation sites (magenta) were stained with
687 Alexa Fluor 488; Scale bar = 20 μm .

688 **Supplemental Figure 1. Different localization of the Fragile X-Related Proteins**
689 **in transzonal projections (TZPs) of porcine cumulus oocyte-complexes (COCs).**
690 Immunofluorescence confocal microscopy images showing the actin filament of the
691 TZP (red) and the presence of FMRP, FXR1P and FXR2P within TZPs (green). Actin
692 filaments of TZPs were stained with Actistain 670 phalloidin (red); primary antibodies
693 against FMRP, FXR1P and FXR2P were subsequently incubated with secondary
694 antibodies conjugated with Alexa Fluor 488 (green). Arrows show some of the
695 granules. Scale bars = 20 μm .

696 **Supplemental Figure 2. Distribution of the cytoplasmic interacting family of FMR**
697 **proteins**

698 **1 and 2 (CYFIP1 and CYFIP2) in porcine cumulus-oocyte complexes (COCs).**

699 Immunofluorescence confocal microscopy images showing the actin filament of the
700 TZP (red) and the localization of A) CYFIP1 and B) CYFIP2 in TZPs (green). TZPs
701 were stained with Actistain 670 phalloidin (red). DNA was stained with Hoechst
702 33432 dye (blue). Primary antibodies against CYFIP1, and CYFIP2 were subsequently

703 incubated with secondary antibodies conjugated with Alexa Fluor 488 (green). Arrows
704 show some of the granules. Scale bars = 20 μ m.

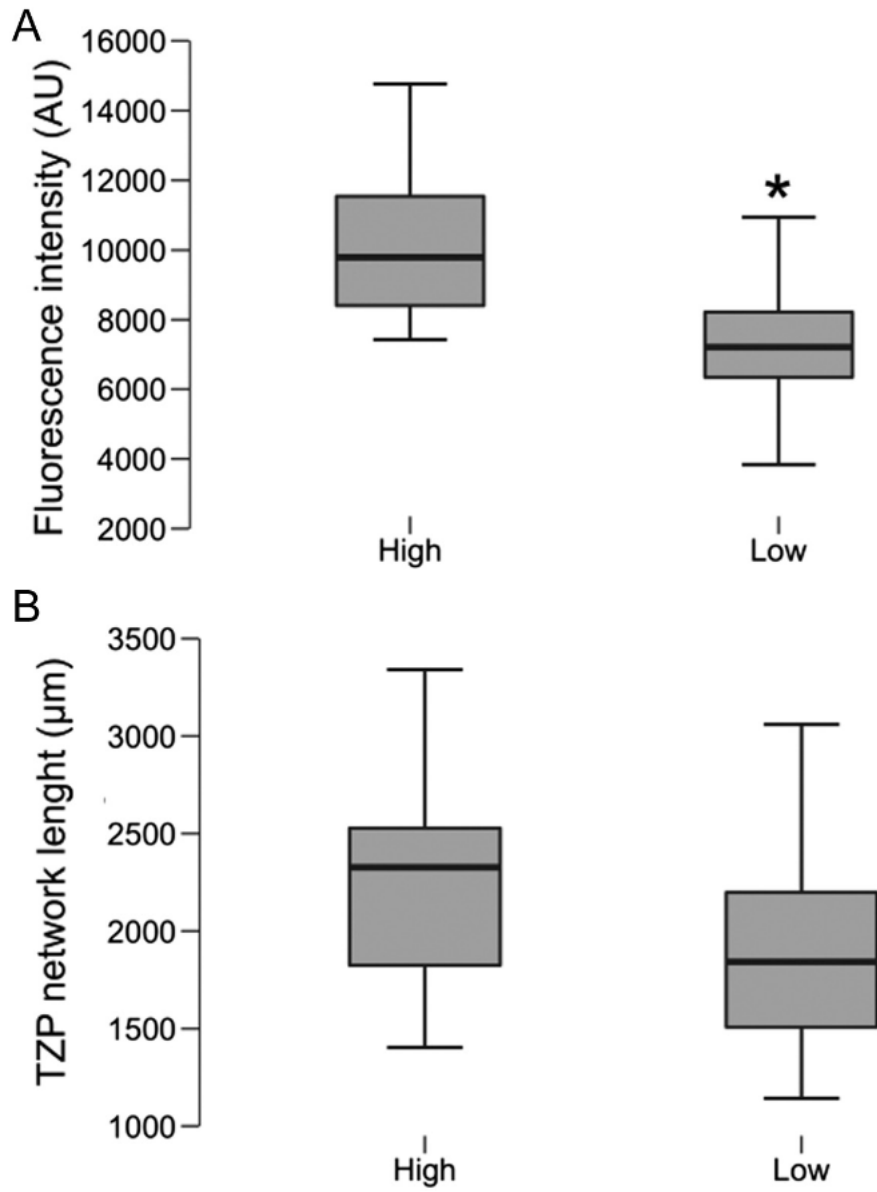
705 **Supplemental Figure 3. Distribution of nuclear interacting FMR protein 1**
706 **(NUFIP1) in porcine cumulus-oocyte complexes (COCs).** Immunofluorescence
707 confocal microscopy images showing the actin filament of the TZP (red) and the
708 localization of NUFIP1 (green) within the TZPs in bovine COCs. TZPs were stained
709 with acti-stain 670 phalloidin (red). Arrows show some of the granules. Scale bars =
710 20 μ m.

711

712

FIGURE 1

713



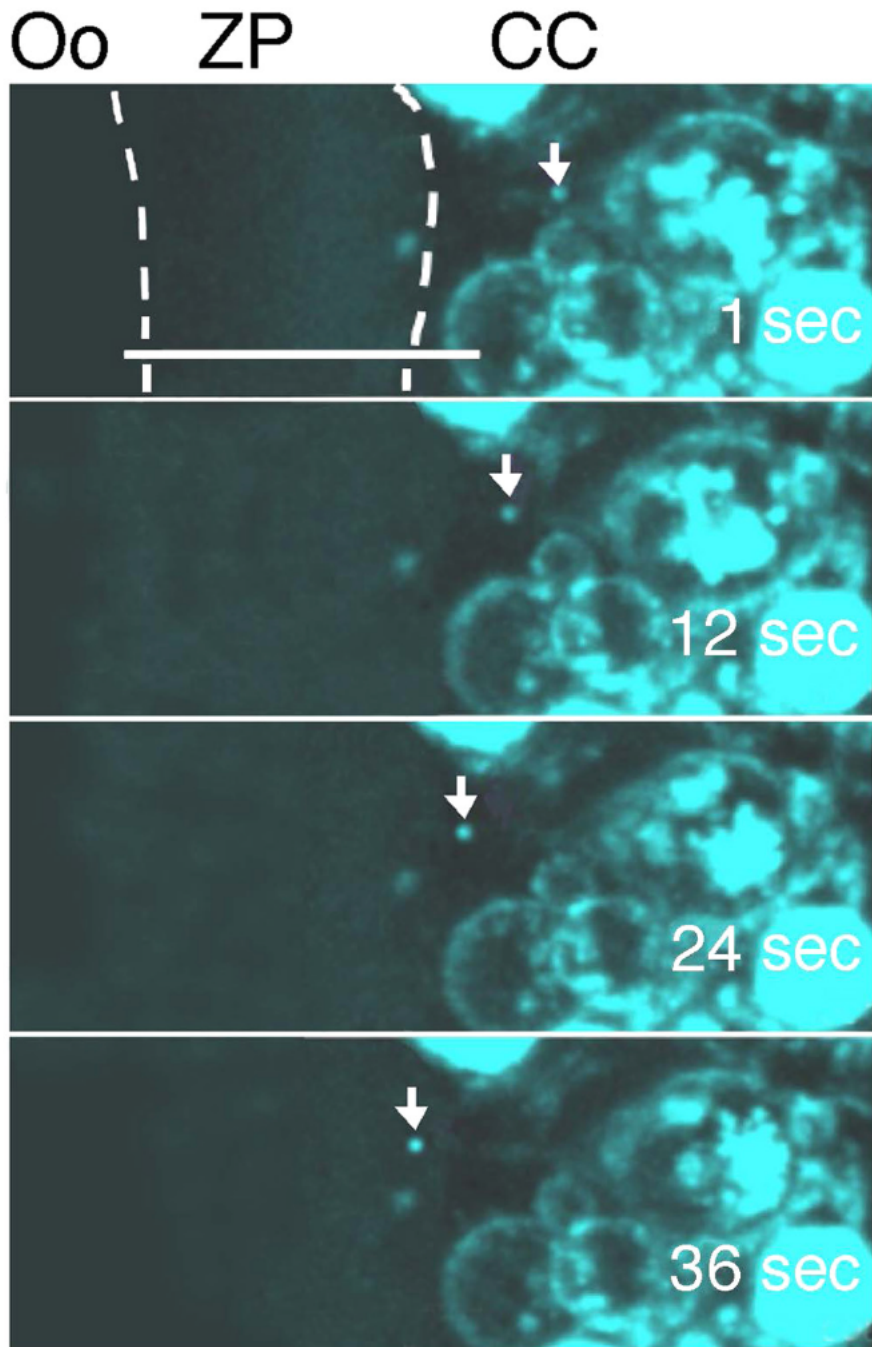
714

715

716

FIGURE 2

717



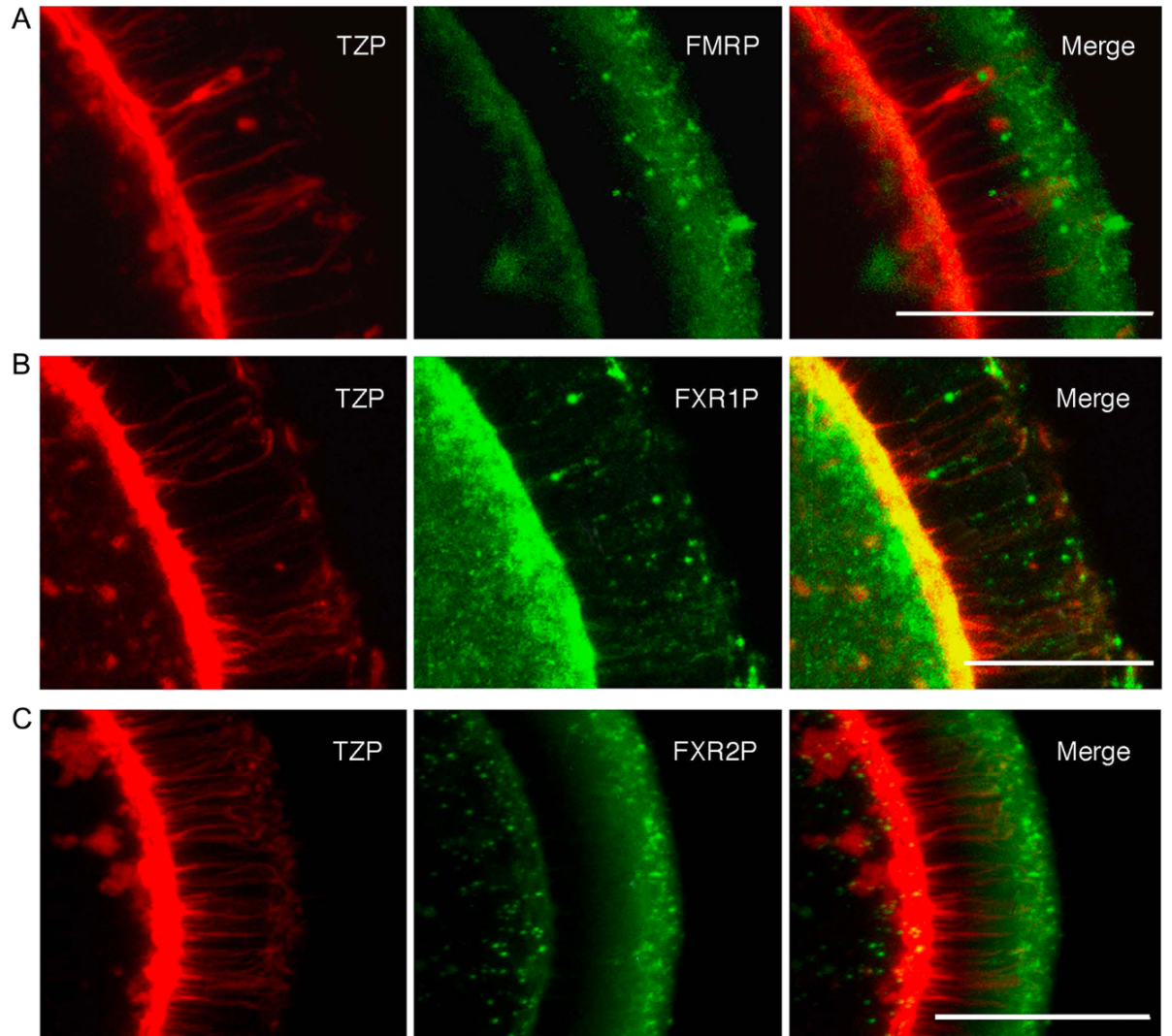
718

719

720

FIGURE 3

721

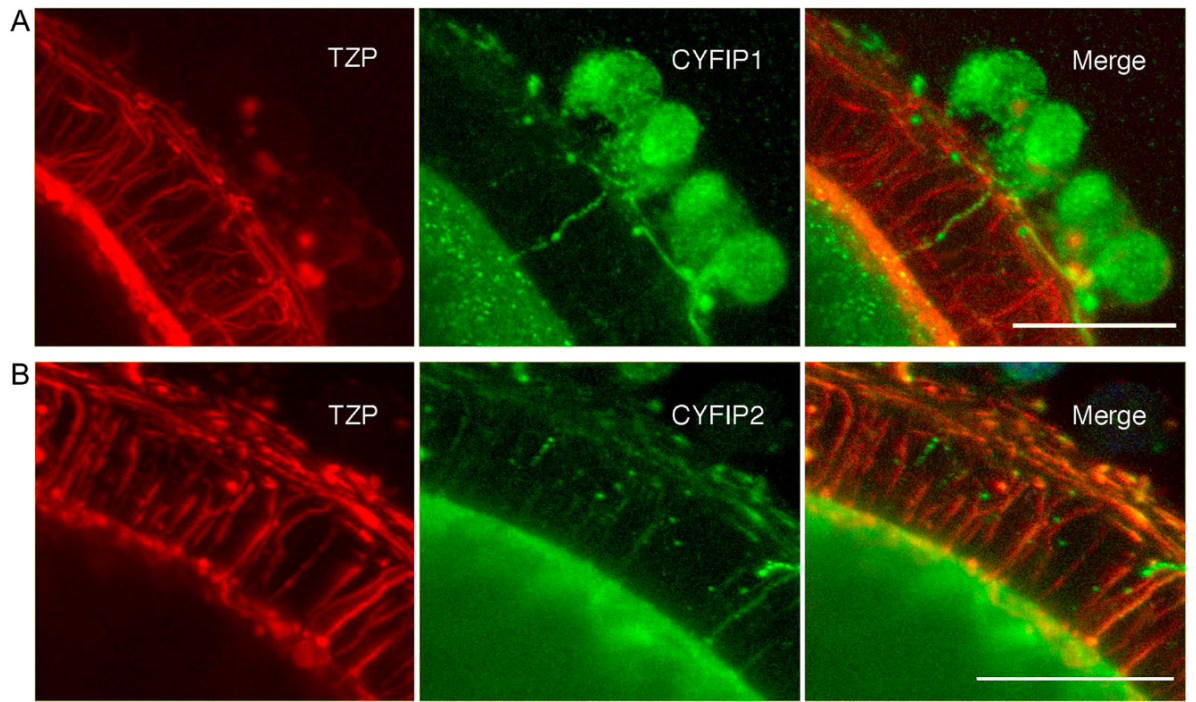


722

723

724

FIGURE 4



725

726

727

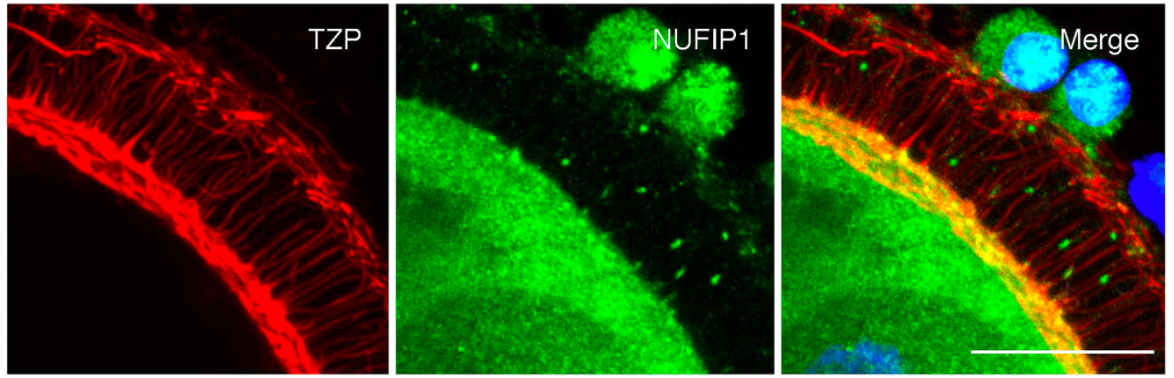
728

729

730

FIGURE 5

731

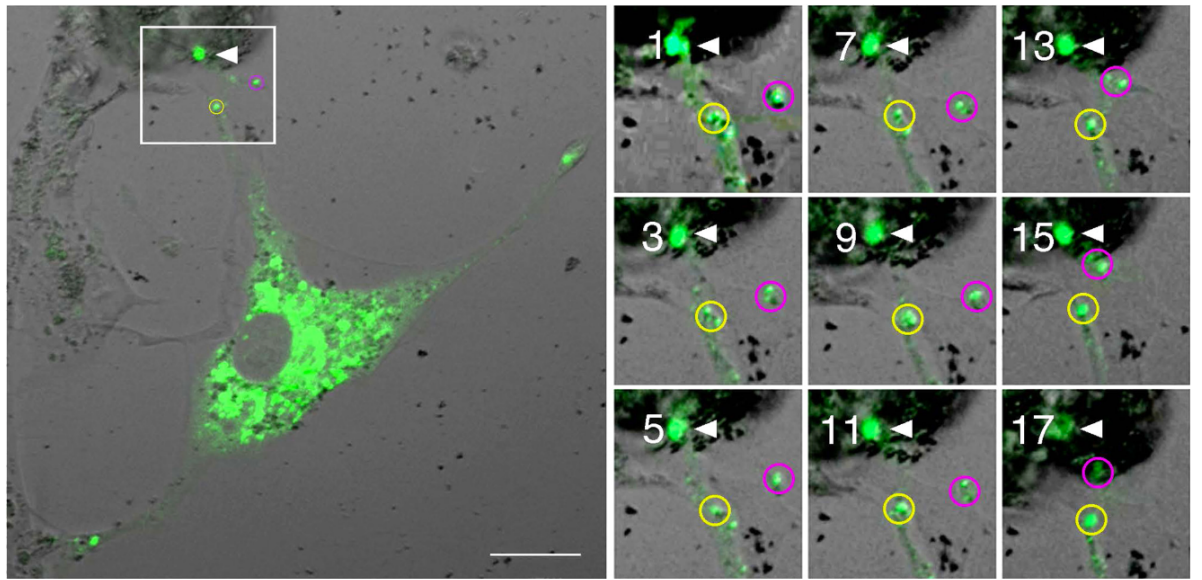


732

733

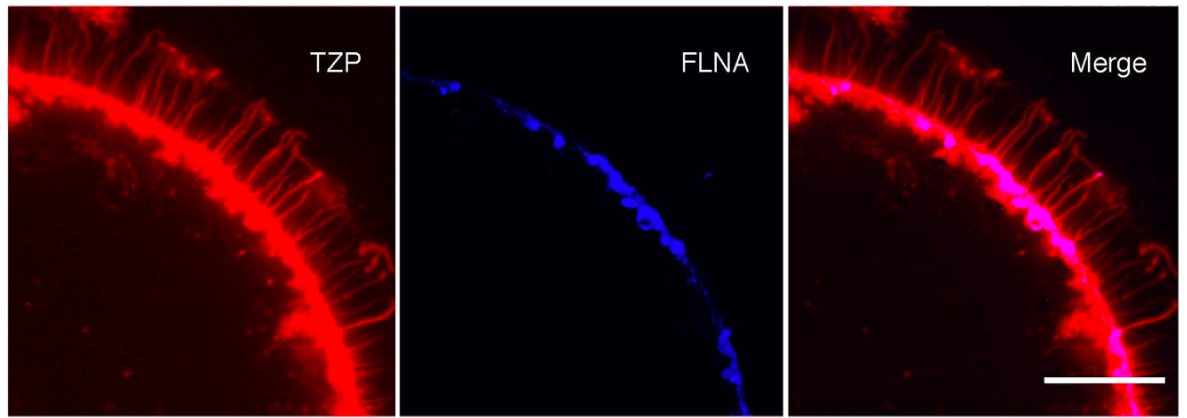
734

FIGURE 6



738

FIGURE 7

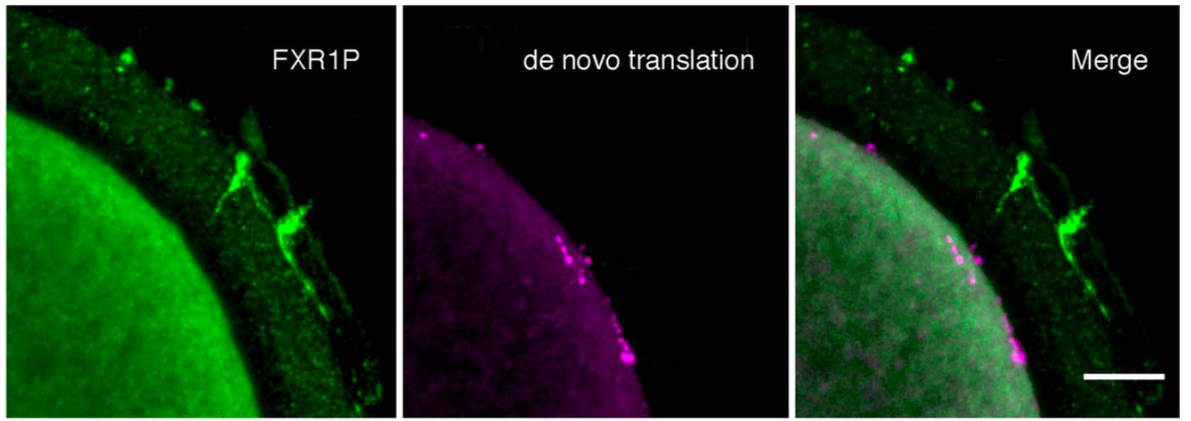


739

740

741

FIGURE 8



742

743

Supplemental Table S1. List of the antibodies used in this study

Antibody Name	Supplier, Catalogue Number	Dilution used in Immunofluorescence	RRID
FMRP	Custom	1:100	
FXR1	Custom	1:1000	
Anti-FXR2, fragile X mental retardation, autosomal homolog 2	Atlas antibodies, HPA022997	1 µg/ml	AB_1849208
CYFIP1 Polyclonal Antibody	Thermo Fisher Scientific, PA5-31984	1 µg/ml	AB_2549457
CYFIP2 Polyclonal Antibody	Thermo Fisher Scientific, PA5-67174	2 µg/ml	AB_2664376
NUFIP1 Polyclonal Antibody	Thermo Fisher Scientific, PA5-56308	1 µg/ml	AB_2644885
Anti-Filamin A Antibody, clone TI10	Millipore, MAB1680	1:100	AB_94323
Goat Anti-Rabbit IgG (H+L) Antibody, Alexa Fluor 488 Conjugated	Thermo Fisher Scientific, A-11008	1:1000	AB_10563748
Rabbit anti-Goat IgG (H+L) Cross-Adsorbed Secondary Antibody, Alexa Fluor 555	Thermo Fisher Scientific, A-21431	1:1000	AB_2535852
Goat Anti-Chicken IgY(H+L) Antibody, CF488A Conjugated	Biotium ,20020-1,	1:1000	AB_10854234